8. J.W. Ryu, S.Y. Kim, and Y.K. Kim, Determination of the optic axis distribution of a hybridly aligned discotic material for wide-view films, J Korean Phys Soc 57 (2010), 233–239.
9. F. Gambou, B. Bayard, and G. Noyel, Characterization of material anisotropy using microwave ellipsometry, Microwave Opt Technol Lett 53 (2011), 1996–1998.
10. M.I.A. Lourakis, A brief description of the Levenberg-Marquardt algorithm implemented by levmar, Found Res Technol 4 (2005), 1–6, 2005.
11. J.-I. Sakai, S. Machida, and K. Tatsuya, Existence of eigen polarization modes in anisotropic single-mode optical fibers, Opt Lett 6 (1981), 496–498.

ALTERNATIVE WAVELENGTH FOR LINEARITY PRESERVATION OF BEER–LAMBERT LAW IN OZONE CONCENTRATION MEASUREMENT

Tay C. E. Marcus,[1] Michael David,[1] Maslina Yaacob,[1,2] Mohd R. Salim,[1] Nabihah Hussin,[1] Mohd H. Ibrahim,[1] Nor H. Ngajikin,[1] Asrul I. Azmi,[1] Sevia M. Idrus,[1] and Zolkafle Buntat[1]
[1] Faculty of Electrical Engineering, Universiti Teknologi Malaysia, 81310 Skudai, Johor, Malaysia; Corresponding author: cemtay2@live.utm.my
[2] Department of Communication Engineering, Faculty of Electrical and Electronic Engineering, Universiti Tun Hussien Onn Malaysia, Parit Raja, 86400 Batu Pahat, Johor, Malaysia

Received 12 September 2014

ABSTRACT: *Beer–Lambert law deviation is often observed. Here, we propose alternative wavelength 279.95 nm for ozone concentration measurement between 357 and 971 μL L^{-1} to preserve linearity. Sensor loses linearity below transmittance 0.2165, as sensor approaches saturation. We recommend measurement of ozone concentration above transmittance of 0.2165 for strong linear relation.* © 2015 Wiley Periodicals, Inc. Microwave Opt Technol Lett 57:1013–1016, 2015; View this article online at wileyonlinelibrary.com. DOI 10.1002/mop.29005

Key words: *Beer–Lambert law; concentration; linearity; ozone; transmittance*

1. INTRODUCTION

Ultraviolet absorption spectroscopy is preferred for ozone concentration measurement recently [1–8]. This is because measurement of absorbance of light is fast and immune to electromagnetic interference. Thus, the technique is safe for measurement of ozone concentration in electrical discharge environment [7, 8]. One common feature of the optical ozone sensors is linearity of measurement. Linearity is an important feature of a sensor for high accuracy measurement, unless the sensor is still at its initial stage of development [6]. Linearity between ozone concentration and natural logarithm of transmittance of light is established in Beer–Lambert law as shown in Eq. (1) [9–11]. Majority measurement results reported in the literature are linear for specific range of concentration. However, in practice, the linearity may not be achieved due to deviation of Beer–Lambert law. For example, linearity of Beer–Lambert law is lost near saturation point [12, 13]. At saturation point, sensor output, natural logarithm of transmittance of light is not responding to change in sensor input, concentration. Deviation of Beer–Lambert law is often observed in previous work. For example, deviation between experiment data and simulation result was observed at high ozone concentration of 0.514 mol m^{-3}, as Beer–Lambert law was presumed to be not applicable for high ozone concentration [14]. This is due to interaction effect at high concentration [15]. Prerequisite of Beer–Lambert law is breached when absorption coefficient, ε or σN_A, becomes a function of concentration, pressure, and absolute temperature [15]. In addition, stray light limits maximum absorption that is possible when light is almost fully absorbed [10]. Furthermore, shadow may be created when light shines on large number of sample molecules, which causes absorbance of light to be smaller than expected [16]. Previous work has attempted to model nonlinear behavior of Beer–Lambert law by considering forward scattering [17]. Scattering effect is found to be prominent at low absorbance [17]. Based on Twyman–Lothian equation, typical transmittance for low relative error of concentration measurement is from 0.25 to 0.50 [11]. There is an optimum transmittance for minimum experiment error for any solution that absorbs light [11]. Based on these facts, we infer that there will be a range of transmittance that disobeys linearity of Beer–Lambert law for ozone concentration measurement.

Deviations of Beer–Lambert law are often modeled and corrected for measurement. However, nonlinearity of measurement still exists. In this letter, we propose an alternative wavelength for measurement of ozone concentration so that linearity of Beer–Lambert law is preserved within specific range of concentration measurement. In addition, we identify range of transmittance that deviates from Beer–Lambert law and recommend suitable range of transmittance to achieve linearity.

2. BEER–LAMBERT LAW AS BASIS OF LINEAR MEASUREMENT

Beer–Lambert law in Eq. (1) shows light intensity decays exponentially when light passes through ozone gas. This is provided temperature, pressure, and concentration are constant.

$$\ln(I_t/I_0) = \ln T_r = -sN_A Plc/\left(10^6 RT\right) \tag{1}$$

c is concentration of ozone in parts per million by volume (μL L^{-1}), I_0 is output intensity without passing through ozone in count, I_t is output intensity that passes through ozone in count, l is optical path length in m, N_A is Avogadro's constant, $6.02214199 \times 10^{23}$ molecule mol^{-1}, P is pressure in atm, R is ideal gas constant, 8.205746×10^{-5} atm m^3 mol^{-1} K^{-1}, T is absolute temperature in K, T_r is transmittance of light that has possible range between 0 and 1 (no unit), σ is absorption cross section of ozone in m^2 $molecule^{-1}$.

3. ABSORPTION CROSS SECTION SIMULATION

Figure 1 shows ozone absorption cross section simulated via spectralcalc.com line list browser from wave number 29,164 to 40,798 cm^{-1} or equivalently from wavelength 254.11 to 342.89 nm. Spectralcalc.com is a subscription-based website for high resolution spectral modeling. The simulation result is reliable because it is based on HITRAN 2008 cross section database. The simulation was done at temperature 300 K and pressure 0 torr. Pattern of simulation result is in good agreement with previous work, which is regarded as highly accurate [18]. We take advantage, the relatively flat peak of ozone absorption cross section at ultraviolet region for sampling wavelength selection. Ozone concentration had been previously measured at 253.65 nm [19–23], 254 nm [4–8], 255 nm [2, 3], and 280 nm [1]. Although ozone concentration is typically sampled at wavelength 253.65 nm for high sensitivity measurement, we propose

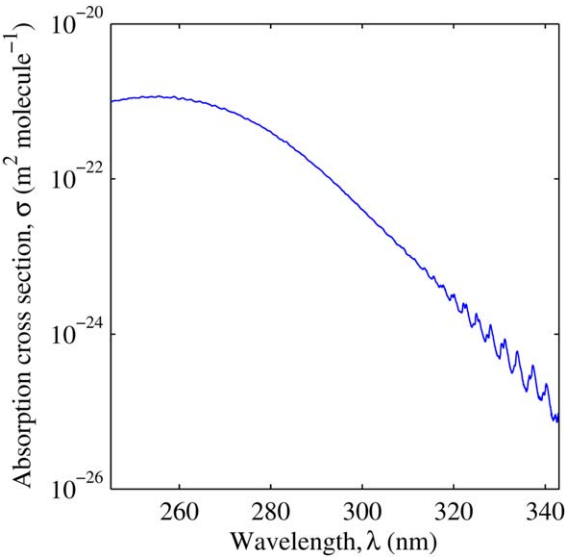

Figure 1 Graph of ozone absorption cross section versus wavelength based on spectralcalc.com simulation. [Color figure can be viewed in the online issue, which is available at wileyonlinelibrary.com]

an alternative wavelength for ozone concentration sampling to preserve linearity of measurement. Figure 1 shows absorption ability of ozone at sampling wavelength 279.95 nm is smaller than typical sampling wavelength 253.65 nm. As Beer–Lambert law is not obeyed at very small transmittance due to saturation, selecting 279.95 nm as sampling wavelength increases transmittance of measurement for the same amount of concentration measured using typical sampling wavelength 253.65 nm. Thus, sampling wavelength 279.95 nm is expected to reduce saturation effect and measure ozone concentration within transmittance range that obeys Beer–Lambert law.

4. EXPERIMENT SETUP

Figure 2 shows experiment setup of this work that consists of optical and gas components. Explanation will begin with optical component. First, Ocean Optics DH-2000 deuterium tungsten halogen light source (1) was switched on to deliver wavelength from 210 to 410 nm to Ocean Optics QP400-025-SR premium solarization resistant fiber of 25 cm length and 400 μm diameter. The use of solarization resistant fiber was necessary to prevent damage of fiber due to ultraviolet radiation. After that, a variable optical attenuator (3) was used to control intensity received at spectrometer so that measurement of light intensity was not saturated. Ocean Optics 74-UV collimating lens (4) were used to focus parallel light beam to and from aluminium gas cell (5). The transmission type aluminum gas cell (5) was custom fabricated at 6.4 mm internal diameter and 10 cm length. Finally, light was received at Ocean Optics HR4000CG-UV-NIR high resolution spectrometer (6) for further analysis using Ocean Optics OceanView software in computer. We measured intensity of light with or without passing through ozone using spectrometer for transmittance calculation. Wavelengths selected for analysis were 253.50, 254.03, 255.10, 260.99, and 279.95 nm, because they were the closest wavelengths measurable by our spectrometer in comparison to previous work [1–8, 19–23]. Wavelength 260.99 nm was the most sensitive wavelength for ozone concentration measurement in this work. Next, gas components will be explained. High purity oxygen supply (99.999% purity) was passed through pressure regulator to regulate flow of oxygen gas to Longevity resources ozone generator EXT50 (7) via vinyl tube. This was to control concentration produced by ozone generator step by step from 357 to 971 μL L^{-1}. Our generator generated minimum 357 μL L^{-1} concentration; whereas, our monitor was certified to measure below 1000 μL L^{-1} concentration. The higher the input flow rate of oxygen to ozone generator, the lower the concentration generated. The ozone generated was supplied via silicone tube to aluminum gas cell (5) for light absorbance. The ozone was terminated at 2B Technologies ozone monitor 106-M (8) for ozone concentration measurement and ozone destruction. Finally, ozone concentration readings were recorded in computer using 2B Technologies Data Display Application software for further analysis using Matlab R2013a software. Temperature of gas cell was monitored using Fluke 54 II B digital thermometer (9).

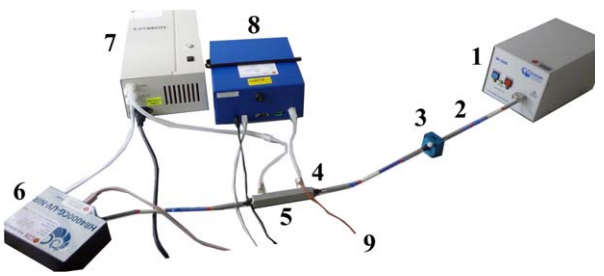

Figure 2 Experiment setup for absorbance measurement based on ozone concentration input. [Color figure can be viewed in the online issue, which is available at wileyonlinelibrary.com]

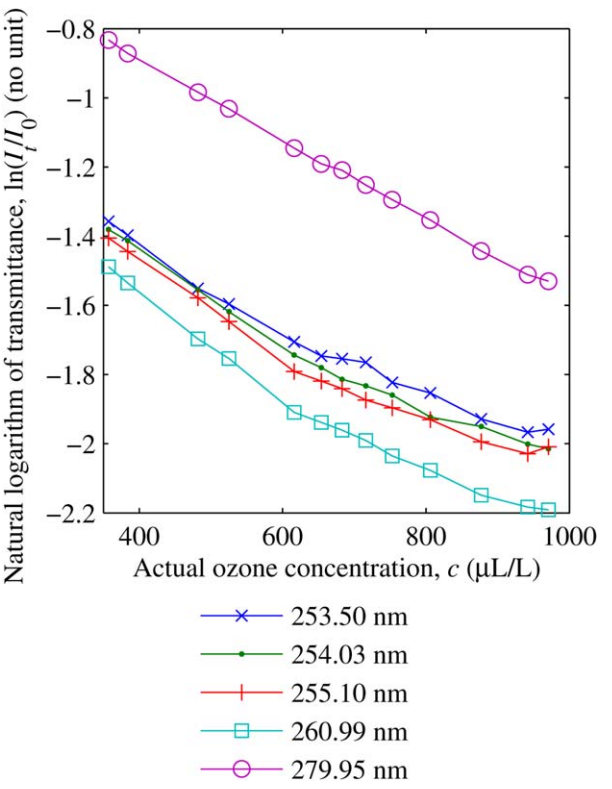

Figure 3 Graph of natural logarithm of transmittance versus actual ozone concentration for various sampling wavelengths based on experiment result. [Color figure can be viewed in the online issue, which is available at wileyonlinelibrary.com]

TABLE 1 Linearity Comparison among Sampling Wavelengths

Wavelength (nm)	Transmittance Range (no unit)	Best Fit Line Based on Linear Regression	Norm of Residuals	Strong Linear Relation
253.50	0.1411–0.2574	$\ln(I_t/I_0) = -0.00098481c - 1.0592$	0.11534	No
254.03	0.1333–0.2513	$\ln(I_t/I_0) = -0.0010412c - 1.0584$	0.12953	No
255.10	0.1341–0.2453	$\ln(I_t/I_0) = -0.0010228c - 1.0994$	0.15819	No
260.99	0.1118–0.2257	$\ln(I_t/I_0) = -0.0011532c - 1.1385$	0.1445	No
279.95	0.2165–0.435	$\ln(I_t/I_0) = -0.0011442c - 0.43229$	0.02218	Yes

5. RESULTS AND DISCUSSIONS

Figure 3 shows graph of natural logarithm of transmittance versus actual ozone concentration for various sampling wavelengths based on experiment result. The negative slope suggests similar pattern to Beer–Lambert law as shown in Eq. (1). However, not all experiment results show strong linear relation. Ideally, Beer–Lambert law suggests a linear graph of constant slope. Besides, wavelength 260.99 nm shows smaller value of natural logarithm of transmittance compared to other wavelengths, because it is the most sensitive wavelength for ozone concentration measurement in this work. However, wavelength 260.99 nm is not recommended for ozone concentration sampling in this work, as sensor approaches saturation at high concentration.

To test linearity of experiment result for various sampling wavelengths, linear regression analysis was done via Matlab R2013a as shown in Table 1. Norm of residuals is a parameter to measure closeness of data points to best fit line, which has zero value in ideal case. According to Table 1, linearity is observed at sampling wavelength 279.95 nm only, because norm of residuals is very small at 0.02218. Other sampling wavelengths 253.50, 254.03, 255.10, and 260.99 nm have large norm of residuals of 0.11534, 0.12953, 0.15819, and 0.1445, respectively, which indicate poor linear fitting. Linearity is observed between transmittance 0.2165 and 0.435 via sampling wavelength 279.95 nm. Transmittance of less than 0.2165 is observed to be not linear for other sampling wavelengths, because sensor approaches saturation when light intensity is almost fully absorbed. The nonlinear behavior at low transmittance may be due to interaction effect [15], stray light [10], and shadow effect [16]. In short, transmittance above 0.2165 is suggested for ozone concentration measurement, due to strong linear relation between sensor input and sensor output.

To verify accuracy of experiment result, values of slope of best fit lines in Table 1 were compared to Beer–Lambert law in Eq. (1) for calculation of absorption cross section. High accuracy absorption cross section calculation is an indicator of high accuracy ozone concentration calculation, as the two parameters are related in Beer–Lambert law in Eq. (1). Average temperature, T of 303.7 K was used for calculation, as temperature of gas cell fluctuated between 303.3 and 304.1 K. Similarly, average pressure, P of 0.9653 atm was used for calculation, as pressure fluctuated between 0.9649 and 0.9658 atm. Optical path length, l of 0.1 m was used for calculation. Table 2 shows comparison of absorption cross section obtained between experiment result and spectralcalc.com simulation. Sampling wavelengths in simulation at 253.4983, 254.0263, 255.102, 260.9876, and 279.9552 nm were selected because they were the closest wavelengths obtainable to sampling wavelengths in experiment at 253.50, 254.03, 255.10, 260.99, and 279.95 nm. Based on Table 2, sampling wavelength 279.95 nm has high accuracy measurement, because small deviation of 20.29% is observed between absorption cross section obtained via experiment and simulation. Other sampling wavelengths 253.50, 254.03, 255.10, and 260.99 nm have large deviation of 62.94, 60.99, 61.88, and 54.65%, respectively, which indicate low accuracy measurement. The large discrepancy between absorption cross section obtained via experiment and simulation may be due to deviation of Beer–Lambert law at low transmittance. Thus, alternative wavelength 279.95 nm is recommended for ozone concentration sampling in this work, due to high accuracy calculation of absorption cross section.

6. CONCLUSIONS AND RECOMMENDATIONS

In conclusion, alternative sampling wavelength 279.95 nm is shown to preserve linearity of Beer–Lambert law for measurement of ozone concentration between 357 and 971 μL L^{-1}. Ten-centimeter transmission type aluminium gas cell was custom fabricated for absorbance measurement in controlled laboratory condition. Comparison between absorption cross section obtained via experiment and spectralcalc.com simulation shows small deviation of 20.29% at sampling wavelength 279.95 nm. However, large deviation of up to 62.94% is observed at sampling wavelength 253.50, 254.03, 255.10, and 260.99 nm, due to deviation of Beer–Lambert law at low transmittance. Linear relation between sensor input and sensor output is not observed below transmittance 0.2165, because sensor approaches saturation. As a result, our recommendation is to measure ozone concentration above transmittance 0.2165 for strong linear relation of Beer–Lambert law and high accuracy calculation of desired parameters.

TABLE 2 Absorption Cross Section Comparison Between Experiment Result and Spectralcalc.com Simulation

Sampling Wavelength in Experiment (nm)	Absorption Cross Section Obtained Based on Experiment, σ_{ex} (m^2 molecule^{-1})	Sampling Wavelength in Simulation (nm)	Absorption Cross Section Obtained Based on Simulation, σ_{sim} (m^2 molecule^{-1})	Deviation, $\lvert\sigma_{ex} - \sigma_{sim}\rvert/\sigma_{sim} \times 100$ (%)
253.50	4.221×10^{-22}	253.4983	1.139×10^{-21}	62.94
254.03	4.463×10^{-22}	254.0263	1.144×10^{-21}	60.99
255.10	4.384×10^{-22}	255.1020	1.150×10^{-21}	61.88
260.99	4.943×10^{-22}	260.9876	1.090×10^{-21}	54.65
279.95	4.904×10^{-22}	279.9552	4.077×10^{-22}	20.29

ACKNOWLEDGMENT

The authors thank Universiti Teknologi Malaysia (UTM) and Ministry of Higher Education (MOHE) Malaysia for supporting this research work under Research University Grant (RUG) Scheme grant no: 05J60 and grant no: 04H35, Fundamental Research Grant Scheme (FRGS) grant no: 4F317, and UTM Zamalah Fellowship.

REFERENCES

1. Y. Aoyagi, M. Takeuchi, K. Yoshida, M. Kurouchi, T. Araki, Y. Nanishi, H. Sugano, Y. Ahiko, and H. Nakamura, High-sensitivity ozone sensing using 280 nm deep ultraviolet light-emitting diode for detection of natural hazard ozone, J Environ Prot 3 (2012), 695–699.
2. M. Degner, N. Damaschke, H. Ewald, S. O'Keeffe, and E. Lewis, UV LED-based fiber coupled optical sensor for detection of ozone in the ppm and ppb range, In: Proceedings of IEEE Sensors Conference, 2009, pp. 95−99.
3. M. Degner, N. Damaschke, H. Ewald, and E. Lewis, High resolution LED-spectroscopy for sensor application in harsh environment: A sensor system based on LED-light sources and standard photodiode receiver is shown as an example of this sensor concept for in-situ gas measurements down to the ppb range, In: Proceedings of IEEE International Instrumentation and Measurement Technology Conference, 2010, pp. 1382−1386.
4. S. O'Keeffe, G. Dooly, C. Fitzpatrick, and E. Lewis, Optical fibre sensor for the measurement of ozone, J Phys Conf Ser 15 (2005), 213–218.
5. S. O'Keeffe, C. Fitzpatrick, and E. Lewis, An optical fibre based ultra violet and visible absorption spectroscopy system for ozone concentration monitoring, Sens Actuators B Chem 125 (2007), 372–378.
6. S. O'Keeffe, M. Ortoneda, J.D. Cullen, A. Shaw, D. Phipps, A.I. Al-Shamma'a, C. Fitzpatrick, and E. Lewis, Development of an optical fibre sensor system for online monitoring of microwave plasma UV and ozone generation system, In: Proceedings of IEEE Sensors Conference, 2008, pp. 454–457.
7. L.D. Maria, G. Rizzi, P. Serragli, R. Marini, and L. Fialdini, Optical sensor for ozone detection in medium voltage switchboard, In: Proceedings of IEEE Sensors Conference, 2008, pp. 1297−1300.
8. L.D. Maria and D. Bartalesi, A fiber-optic multisensor system for predischarges detection on electrical equipment, IEEE Sens J 12 (2012), 207–212.
9. I.M. Campbell, Energy and the atmosphere: A physical-chemical approach, 2nd ed., Wiley, New York, NY, 1986.
10. B.J. Clark, T. Frost, and M.A. Russell, Techniques in visible and ultraviolet spectrometry volume 4: UV spectroscopy, techniques, instrumentation, data handling, Chapman & Hall, London, UK, 1993.
11. H.K. Hughes, Beer's law and the optimum transmittance in absorption measurements, Appl Opt 2 (1963), 937–945.
12. K. Fuwa and B. L. Valle, The physical basis of analytical atomic absorption spectrometry. The pertinence of the Beer–Lambert law, Anal Chem 35 (1963), 942–946.
13. M. Yasin, S.W. Harun, C.F. Tan, S.W. Phang, and H. Ahmad, Fiber optic chemical sensor using fiber coupler probe based on intensity modulation for alcohol detection, Microwave Opt Technol Lett 53 (2011), 1935–1938.
14. Q. Yang, S.O. Pehkonen, and M.B. Ray, Performance evaluation of light emission models in light attenuating media, Ozone Sci Eng 27 (2005), 459–467.
15. R.J. Brock, A note on the Beer–Lambert law, Anal Chim Acta 27 (1962), 95–97.
16. M.L. Larsen and A.S. Clark, On the link between particle size and deviations from the Beer–Lambert–Bouguer law for direct transmission, J Quant Spectrosc Radiat Transf 133 (2014), 646–651.
17. L. Wind and W.W. Szymanski, Quantification of scattering corrections to the Beer–Lambert law for transmittance measurements in turbid media, Meas Sci Technol 13 (2002), 270–275.
18. E.C.Y. Inn and Y. Tanaka, Absorption coefficient of ozone in the ultraviolet and visible regions, J Opt Soc Am 43 (1953), 870–873.
19. J. Brion, A. Chakir, D. Daumont, J. Malicet, and C. Parisse, High-resolution laboratory absorption cross section of O3, Temperature effect, Chem Phys Lett 213 (1993), 610–612.
20. D. Daumont, J. Brion, J. Charbonnier, and J. Malicet, Ozone UV spectroscopy I: Absorption cross-sections at room temperature, J Atmos Chem 15 (1992), 145–155.
21. A.G. Hearn, The absorption of ozone in the ultra-violet and visible regions of the spectrum, Proc Phys Soc 78 (1961), 932–940.
22. J. Malicet, D. Daumont, J. Charbonnier, C. Parisse, A. Chakir, and J. Brion, Ozone UV spectroscopy, II. Absorption cross-sections and temperature dependence, J Atmos Chem 21 (1995), 263–273.
23. S. Voigt, J. Orphal, K. Bogumil, and J.P. Burrows, The temperature dependence (203–293 K) of the absorption cross sections of O3 in the 230–850 nm region measured by Fourier-transform spectroscopy, J Photochem Photobiol A Chem 143 (2001), 1–9.

AN INTEGRATED "SENSE-AND-COMMUNICATE" BROAD-/NARROW-BAND OPTICALLY CONTROLLED RECONFIGURABLE ANTENNA FOR COGNITIVE RADIO SYSTEMS

XiongYing Liu,[1] Yi Fan,[1] and Manos M. Tentzeris[2]
[1] School of Electronic and Information Engineering, South China University of Technology, Guangzhou 510640, China; Corresponding author: liuxy@scut.edu.cn
[2] School of Electrical and Computer Engineering, Georgia Institute of Technology, Atlanta, Georgia 30332

Received 13 September 2014

ABSTRACT: *An optically controlled reconfigurable antenna with operability in both wide and narrow bands is investigated for cognitive radio systems. The proposed antenna consists of a U-shaped patch for the spectrum sensing over a wide band and two open annuli for communication in narrow sub-bands within the frequency range of 3.1–10.6 GHz. The integration of narrow and wide bands devices makes the whole antenna structure compact with a dimension of 40 × 38.5 mm^2. With an inherent property of being electromagnetically transparency, four appropriately placed laser-controlled photoconductive silicon switches are adopted to achieve reconfigurable frequency characteristics in the four bands of 5.8–6.8, 6.7–7.3, 7.0–8.4, and 7.9–9.2 GHz with the reflection coefficient below -10 dB. The wide-narrowband antenna is fed by two coplanar waveguides with the isolation of $S_{21} < -15$ dB, effectively allowing the spectrum sensing and the communication to operate simultaneously. An antenna prototype has been fabricated, and close agreement is observed between the measured and simulated results.* © 2015 Wiley Periodicals, Inc. Microwave Opt Technol Lett 57:1016–1023, 2015; View this article online at wileyonlinelibrary.com. DOI 10.1002/mop.29004

Key words: *Frequency reconfigurable antenna; cognitive radio; optical control; photoconductive switches*

1. INTRODUCTION

With the increasing demand for wireless communications, the radio frequency spectrum has become a scarce resource. Nevertheless, some frequency bands in the spectrum, especially above 3 GHz, are partially unoccupied at most of the time [1]. However, according to the fixed spectrum access (FSA) policy [2], unauthorized users are not allowed to operate at the licensed spectrum. To improve the management and utilization of the radio spectrum, the Federal Communications Commission